Desalination and Water Treatment
www.deswater.com

doi: 10.5004/dwt.2020.24922

175 (2020) 108–114
January

Nonylphenol ethoxylate-assisted hydrothermal preparation of carbon adsorbent from phenolic waste liquid

Qu Chen[a], Wenqi Zhang[a,b,*], Pinhua Rao[a], Runkai Wang[a]

[a]*College of Chemistry and Chemical Engineering, Shanghai University of Engineering Science, Shanghai, 201620, China, Tel. +86-159-0074-6789; Fax +86-021-6779-1214; email: zhangwenqi_hit@163.com (W. Zhang), Tel. +86-150-2673-8669; email: 330083117@qq.com (Q. Chen), Tel. +86-021-6779-1211; email: raopinhua@hotmail.com (P. Rao), Tel. +86-136-2172-0394, email: wrk007@163.com (R. Wang)*
[b]*School of Civil Engineering, Kashi University, Kashi, 844006, China*

Received 23 April 2019; Accepted 16 September 2019

ABSTRACT

Phenolic waste liquid is produced from the distillation of high-concentration phenolic wastewater, and must be treated as hazardous waste. Converting this waste liquid to hydrochars is a good way of resource utilization. However, doing this is difficult for the hydrothermal carbonization process at lower temperature. In this work, in the presence of sulfuric acid, nonylphenol ethoxylate can effectively assist the hydrochar formation from phenolic waste liquid at 180°C. The hydrochars were characterized by an elemental analyzer, scanning electron microscope (SEM), surface area, pore volume and size, and Fourier transform infrared spectrometer. At the optimal condition, the hydrochar showed great methylene blue (MB) adsorption capacities, and the maximum adsorption capacity was 698 mg g^{-1} according to Langmuir isotherms, which is higher than that of commercial activated carbon (i.e., 363 mg g^{-1}). Thus, the hydrochar could be a promising adsorbent for wastewater treatment.

Keywords: Phenolic waste liquid; Nonylphenol ethoxylate; Hydrothermal carbonization; Adsorbent

1. Introduction

High-concentration phenolic wastewater is produced in various industries and not conducive to biodegradation because of its high toxicity to the microbial population [1]. Many physical and chemical methods, such as incineration [2], distillation [3], extraction [4,5], wet–air oxidation [6,7], electrochemical oxidation [8,9], and ion exchange [10], have been proposed for phenolic wastewater treatment. However, these technologies still have many challenging problems, such as extractant loss, high energy consumption, low efficiency, and secondary pollution.

Wastewater distillation has the disadvantage of high energy consumption. However, this process can remarkably reduce the amount of wastewater discharged and can be used to treat high-concentration phenolic wastewater under a highly basic condition by some enterprises. The distilled water can be treated by biotechnology because of its low phenol concentration, but the distilled residues, that is, phenol waste liquid, are difficult to deal with.

Hydrothermal carbonization (HTC) is a novel thermal conversion process that can be a viable means for treating waste streams while minimizing greenhouse gas production and producing residual material with an intrinsic value [11]. The preparation of carbon materials from the HTC of biomass has been widely used because of its simplicity, low cost, greenness, and high efficiency [12–17]. The carbonization of organic pollutants by this process has attracted attention in recent years, but no report on the treatment of phenolic waste

* Corresponding author.

liquid has been presented. Nevertheless, many literatures have mentioned the transformation characteristics of phenol during HTC or pyrolysis of biomass, and phenol was found to be hardly converted into carbon materials at lower temperatures [18–22]. For example, Weiner et al. [23] reported that under harsh HTC reaction conditions (255°C for 16 h), bisphenol A (BPA) was quantitatively converted, but phenol was identified by gas chromatography–mass spectrometry (GC–MS) analysis as the transformation products [23]. In our previous work, phenolic waste liquid was not successfully carbonized by HTC at 180°C–220°C for 4–8 h under a highly acidic condition.

Catalysts can increase the rate of chemical reactions by reducing the activation barrier. Many chemicals, such as acid [24,25], alkali [24–26], metal ions [27], metal chlorides [28–31], and sucrose [23], can be used to improve the HTC of biomass from the viewpoint of energy consumption or quality of products.

Nonylphenol ethoxylate is a kind of nonionic surfactant largely used in many agricultural and industrial applications. A previous work showed that nonylphenol ethoxylate can be effectively converted to porous carbon via HTC at 180°C for 4 h under acidic conditions (maintain a 2:1 sulfuric acid: nonylphenol ethoxylate ratio) [32]. This study aims to examine the assisted performances of nonylphenol ethoxylate in the HTC of phenolic waste liquid.

2. Materials and methods

2.1. Materials

Phenolic waste liquid was supplied by a company in Zhejiang Province. The COD and the total phenol content of the sample were 143 and 43.5 g L^{-1}, respectively. Phenol (AR) was purchased from Yonghua Chemical Technology (Jiangsu) Co., Ltd. Nonylphenol ethoxylate (NP-10) was purchased from Lvsen Chemical Co., Ltd. (No. 426, Area A, Lunan Chemical Market, Lanshan District, Linyi City, Shandong Province, China) with 99% active substance content. Sulfuric acid (AR, 98%) and activated carbon (AR, 200 mesh) were purchased from Shanghai Titan Scientific Co., Ltd. Methylene blue (C16H18ClN3S·3H2O) was purchased from Sinopharm Chemical Reagent Co., Ltd.

2.2. Hydrothermal carbonization experiment

The HTC experiments were performed in 50 mL polytetrafluoroethylene (PTFE) lined stainless steel autoclave reactor (Binhai, Jiangsu, China). The dosages of phenolic waste liquid and sulfuric acid (98%) were 2 and 4 mL, respectively. Table 1 shows the dosages of NP-10. The temperature ramped at a rate of 5°C min^{-1} from room temperature to the desired value (180°C) under autogenous pressure when the HTC treatment started. The carbonization time of 4 h was maintained when the preset temperature was reached.

The reaction vessels were cooled to room temperature naturally after the HTC treatment. The hydrochars were then washed by 50 mL distilled water and filtered through a quantitative filter paper (medium speed). The hydrochars were dried in an oven at 120°C for 2 h after the separation. Its yield (g) was weighed with an analytical balance, then stored in a desiccator before further analysis.

The analytical procedures for COD were performed according to the potassium dichromate method and standard methods issued by the State Environmental Protection Administration of China (2002) [33]. Phenol was analyzed by high-performance liquid chromatography (HPLC) (LC–2030, Shimadzu International Trading Co. Ltd., Shanghai) equipped with a quaternary pump and a UV detector at 270 nm. An auto-sampler was used to inject samples (20 μL) into an Ultimate AQ-C18 column (5 μm, 4.6 × 150 mm) at 40°C. The mobile phase composition was 20% distilled water and 80% methanol, and the mobile phase flow rate was 1.0 mL min^{-1}.

2.3. Characterization methods of hydrochars

The elemental composition of hydrochars was analyzed using an elemental analyzer (Vario EL III, Germany). The surface morphological characteristics and hydrochar structure were characterized using a scanning electron microscope (SEM) (HITACHI S–3400, Japan). The N_2 adsorption–desorption isotherms were collected on Micromeritics ASAP 2460 (4356 Communications Drive, Norcross, GA 30093-2901, U.S.A.) at a temperature of 77 K, from which, the surface area (S_{BET}), pore volume (V_p) and pore diameter (D_p) were determined by applying

Table 1
Yield and elemental analysis of hydrochars, phenol concentration, and COD of the washing water[a]

Sample code[b]	NP-10 dosage (mL)	Yield (g)[c]	Elemental composition (wt.%)			Phenol concentration (mg L^{-1})[d]	COD (mg L^{-1})
			C	H	N		
HC1	2	1.62	67.85	6.21	<0.05	n.d.	698
HC2	1	0.88	60.78	5.23	<0.05	n.d.	514
HC3	0.2	0.27	51.57	4.62	<0.05	n.d.	387
HC4	0.1	0.18	47.64	4.58	<0.05	n.d.	350
HC5	0.075	0.16	46.53	4.55	<0.05	n.d.	499
HC6	0.05	0.10	41.71	4.68	<0.05	n.d.	1641

[a]Washing water: included the reaction solution.
[b]HC1–HC6: hydrochars prepared from the hydrothermal carbonization of phenolic waste liquid in the presence of sulfuric acid and different NP-10 dosages at 180°C for 4 h.
[c]Yield (g): mass of hydrochars weighed with an analytical balance.
[d]n.d.: not detected.

the Brunauer–Emmett–Teller (BET) and Barrett–Joyner–Halenda (BJH) models from the desorption branches. The functional groups on the hydrochar surface were detected using Fourier transform infrared spectrometer (FTIR) (Nicolet AVATAR 370, USA) in the infrared range between 4,000 and 400 cm^{-1}.

2.4. Methylene blue (MB) adsorption experiments

The MB adsorption from the aqueous solution using hydrochars was achieved according to the batch experiments performed in a temperature-controlled shaker at 150 rpm and 20°C. The hydrochars were screened by 200 mesh sieves. The adsorption kinetics was performed in the previous experiment. The optimum adsorption time was 120 min, while the optimum pH of wastewater was 6.0.

In the experiments, 0.02 g of hydrochars was included into the 1 L of MB solutions at desired concentrations. The MB concentration was measured at 664 nm using a UV–Vis spectrophotometer (UV-5100, Shanghai Metash Instruments Co., Ltd., No. 9, Lane 1276, Nanle Road, Songjiang District, Shanghai, China). The desired concentration of the methylene blue solutions was obtained through the stock solution dilution (1,000 mg L^{-1}) with distilled water. The MB concentration that remained unadsorbed in the solution was determined, and the amount of MB adsorbed per gram of hydrochar was calculated using the following formula [34]:

$$q_e = \frac{(C_0 - C_e)V}{m} \quad (1)$$

where q_e (mg g^{-1}) is the amount of MB adsorbed per gram of hydrochars; C_0 (mg L^{-1}) is the initial MB concentration; C_e (mg L^{-1}) is the concentration of MB that remained unadsorbed in the solution; V (mL) is the volume of the MB solution; and m (g) is the amount of hydrochars.

3. Results and discussion

3.1. HTC results in different conditions

The experimental results showed that all samples (HC1–HC6) were successfully carbonized under the given experimental conditions, indicating that the addition of NP-10 was greatly beneficial to the carbonation of phenolic waste liquid. Table 1 shows the yield of the hydrochars, phenol concentration and COD of washing water of all samples. However, the yield of the experimentally obtained hydrochars included the hydrochar yield obtained via HTC of NP-10 and phenolic waste liquid. NP-10 was used as the feedstock to study the yield of hydrochars under the same conditions; the corresponding hydrochar yields were 1.55, 0.80, 0.18, 0.10, 0.072, and 0.038 g, respectively. Therefore, the hydrochar yield of the phenolic waste liquid, which is the difference between the hydrochar yield obtained experimentally and that obtained from NP-10 carbonization, was 0.07, 0.08, 0.09, 0.08, 0.088, and 0.062 g, respectively.

Table 1 presents the elemental composition of hydrochars. The carbon content of the hydrochars was high, as expected. Although NP-10 can assist the phenol carbonization, the C content of the hydrochars continuously decreased, which was mainly attributed to the decreasing dosage of NP-10, indicating that the hydrochar quality was degraded. Phenol may not be carbonized if the NP-10 dosage is further reduced. The secondary pollution of this process for phenolic waste liquid treatment was not serious. The washing water was subjected to HPLC, and no phenol was detected, illustrating that phenol was completely degraded during the HTC process. The washing water was tested by GC–MS (QP–2010, Shimadzu, Japan), and the experimental results showed that the washing water comprised the main components such as ethanoic acid, ethyl sulfate and ethyl propanoate. The COD of the washing water of HC1 and HC6 was higher than that of the other samples, which was corresponding to the hydrochar yield of the phenolic waste liquid feedstock.

3.2. SEM analysis

Fig. 1 shows the SEM images of the hydrochars. The NP-10 dosage affected the surface morphology of the hydrochars, with the occurrence of significant structural changes. Dense carbon spherules (5–10 μm) were observed for the HC1 and HC2 samples. Moreover, some of the small-sized flake, columnar, and needle-like particles were produced on the sphere surface.

A very similar surface appearance was exhibited for the HC3, HC4, and HC5 samples with the decrease of the NP-10 dosage. More irregular small particles (0.1–0.5 μm) appeared on the hydrochar surface and aggregated to a porous structure. The hydrochar morphology was still porous when the NP-10 dosage decreased to 0.05 mL (Fig. 1, HC6). However, compared with that of the other samples, the HC6 surface was smoother and denser, which were not conducive to the pore development.

3.3. Surface area and pores

Fig. 2 presents the N_2 adsorption–desorption isothermals of the HC3, HC4, HC5, and HC6 samples. All isotherms of these samples emerged a sharply upswept rear edge at a high relative pressure ($P/P_0 > 0.9$) corresponding to the macroporous adsorption and type-II sorption behavior according to the IUPAC classifications [35]. No obvious adsorption–desorption hysteresis loops for these samples were observed, particularly for samples HC4 and HC5. The adsorption and desorption branches of the isotherm coincided. The BET surface areas, pore volume, and pore diameter (Table 2) were estimated by the BET equation and the BJH model. The hydrochars (HC1, HC2) showed a very low amount of adsorbed gas when NP-10 was the main feedstock, indicating the lack of a developed porosity. The BET specific surface area and the pore volume were 0.78–1.28 $m^2\ g^{-1}$ and 0.003 $cm^3\ g^{-1}$, respectively. The specific surface area and the pore volume of the hydrochars (i.e., HC3, HC4, HC5) significantly increased with the decrease of the NP-10 dosage. In addition, the maximum specific surface area could reach 14.05 $m^2\ g^{-1}$. However, for sample HC6, the specific surface area and pore volume decreased, and the pore size further decreased when the NP-10 dosage was reduced to 0.05 mL. The right amount of surfactant contributed to the pore formation of the hydrochars produced from phenolic waste liquid.

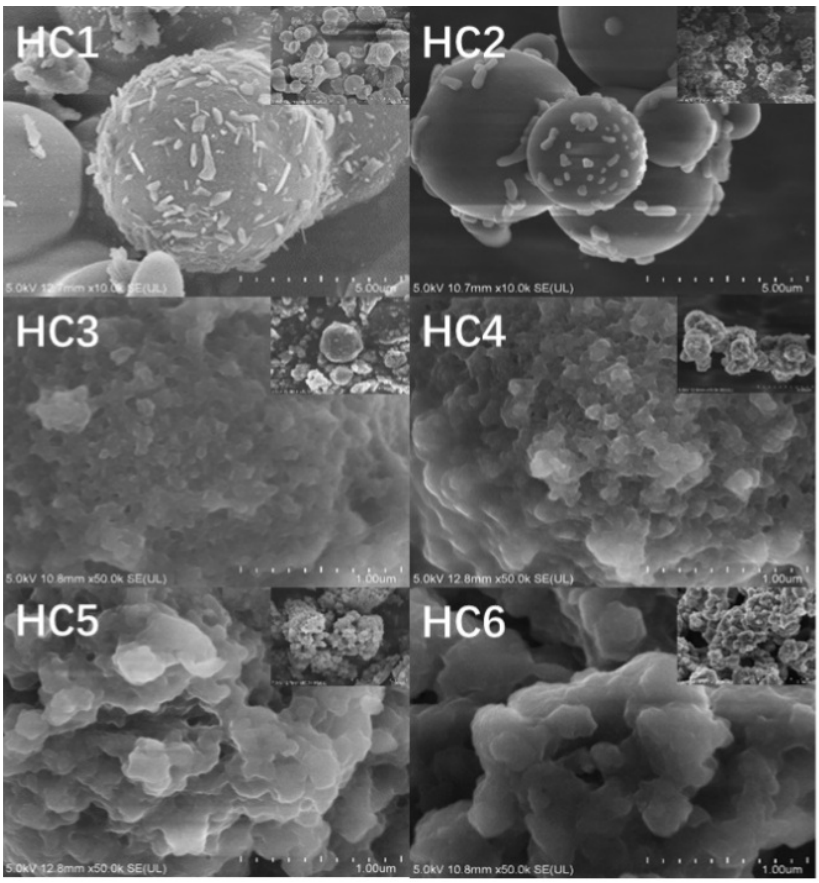

Fig. 1. SEM images of the hydrochars.

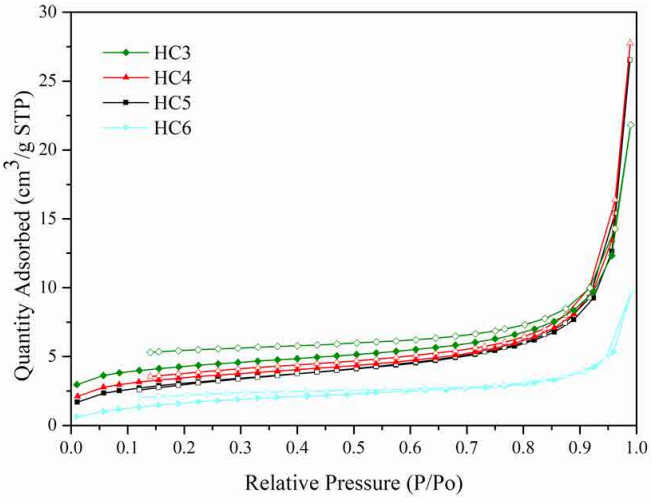

Fig. 2. N_2 adsorption–desorption isotherms of HC3, HC4, HC5, HC6.

Table 2
Structural parameters of the hydrochars

Sample code	S_{BET} ($m^2 g^{-1}$)[a]	V_p ($cm^3 g^{-1}$)[b]	D_p (Å)[c]
HC1	0.78	0.003	281
HC2	1.28	0.003	299
HC3	10.73	0.030	172
HC4	11.70	0.040	190
HC5	14.05	0.041	216
HC6	6.31	0.015	102

[a]S_{BET} is BET surface area.
[b]V_p is pore volume.
[c]D_p is pore diameter.

3.4. FTIR analysis

The organic functional groups in HC3, HC4, HC5, HC6, and activated carbon (AC) were characterized via the FTIR analysis (Fig. 3). The types of functional groups on the hydrochars were richer than that on the AC, indicating that it had a better adsorption potential. The peak at 3,350–3,450 cm^{-1} belonged to the vibration of the O–H stretching, showing that the substantial numbers of the –OH groups were on the hydrochar surface [36]. The peaks from 2,800 to 3,000 cm^{-1} were assigned to the aliphatic C–H vibration [37]. The peak at 1,604 cm^{-1} was characteristic of the C=O stretching vibration of the carbonyl groups [38]. The peak at 1,100–1,300 cm^{-1} indicated C–O, C–OH, and O–H stretching vibrations [39,40]. The peaks visible at the 1,000–1,100 cm^{-1} band suggested the presence of the sulfonic acid group [41]. The bands near 880 and 610 cm^{-1} were attributed to the aromatic C–H

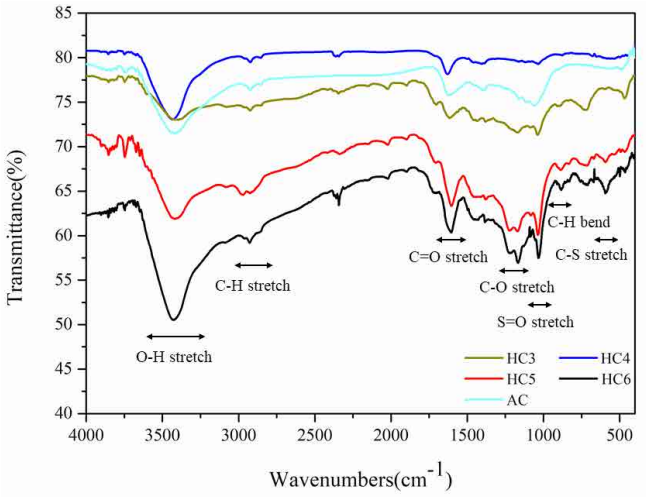

Fig. 3. FTIR spectra of HC3, HC4, HC5, HC6, and AC.

out-of-plane bending and C–S stretching vibrations, respectively [32]. Above all, these results indicated that aromatization occurred during HTC.

3.5. MB adsorption isotherms

The isotherm analysis was performed and drew support from the Langmuir [42] and Freundlich [43] isotherm models defined by the following equations, respectively.

$$q_e = \frac{q_{\max} K_L C_e}{1 + K_L C_e} \tag{2}$$

$$q_e = K_F C_e^{\frac{1}{n}} \tag{3}$$

where q_e (mg g^{-1}) is the amount of MB adsorbed per gram of hydrochars; C_e (mg L^{-1}) is the concentration of MB that remained unadsorbed in the solution; K_L (L mg^{-1}) and $q_{\max}$ (mg g^{-1}) are the Langmuir constants related to free energy or adsorption enthalpy and maximum monolayer adsorption capacity, respectively; and the Freundlich coefficients n and K_F are related to the adsorption intensity and capacity, respectively.

The amounts of MB adsorbed per gram of HC3, HC4, HC5, and HC6 were 527, 491, 698, and 502 mg g^{-1}, respectively, which were larger than that of the AC for MB adsorption (363 mg g^{-1}). The adsorption capacity of HC5 was the largest when compared with HC3, HC4, and HC6. Fig. 4 shows the Langmuir and Freundlich isotherms plotted for MB adsorption on HC5 and AC. Table 3 presents the isotherm coefficients of both models. The correlation coefficient of the Langmuir isotherm model was larger than that of the Freundlich isotherm model, indicating that the Langmuir isotherm model was better fitted with the experimental data [34,44].

3.6. Adsorption kinetics

Fig. 5 shows the adsorption kinetics of HC5. The results showed that rapid adsorption occurred at the initial 10 min, which can be ascribed to the large number of active sites on the surface of HC5 at this initial stage. Adsorption also reached an equilibrium in approximately 120 min.

The kinetic analysis of the experimental data was achieved through pseudo-first order [45] and pseudo-second

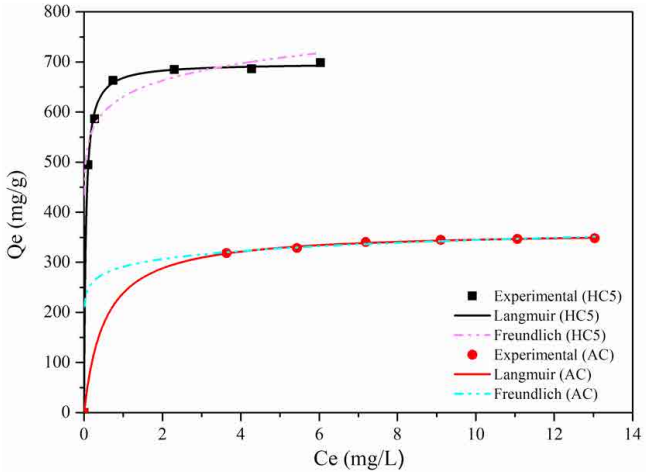

Fig. 4. Experimental, Langmuir, and Freundlich isotherm graphs for adsorption of MB by HC5 and AC at 20°C (pH: 6.0; initial MB concentration: 10–20 mg L^{-1}; HC5 dosage: 0.02 g; volume of MB solution: 1 L).

Table 3
Parameters of Langmuir and Freundlich isotherms for MB adsorption by HC5 and AC

Sample code	Langmuir isotherm model			Freundlich isotherm model		
	$Q_{\max}$ (mg g^{-1})	K_L (L mg^{-1})	R^2	K_F (mg g^{-1})	n	R^2
HC5	697.65	22.62	0.9992	630.74	13.89	0.8135
AC	363.26	1.91	0.9998	291.34	13.71	0.9344

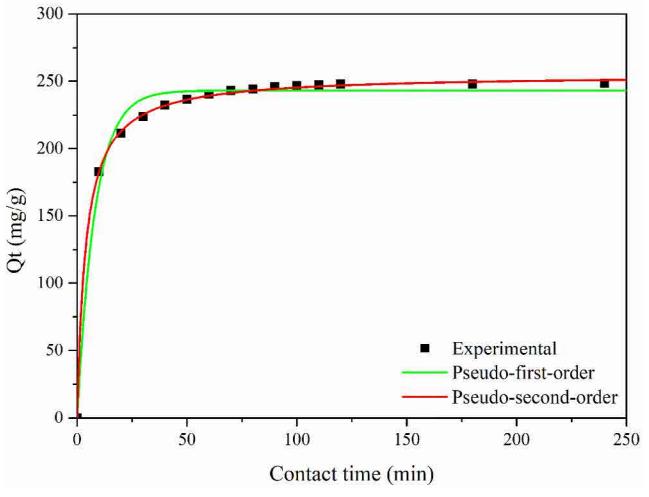

Fig. 5. Effect of contact time on MB adsorption by HC5 at 20°C (pH: 6.0; initial MB concentration: 5 mg L^{-1}; HC5 dosage: 0.02 g; volume of MB solution: 1 L).

Table 4
Parameters of pseudo-first order and pseudo-second order kinetic models for MB adsorption by HC5

C_0 (mg L^{-1})	Pseudo-first order kinetic model			Pseudo-second order kinetic model		
	k_1 (min^{-1})	q_e (mg g^{-1})	R^2	k_2 (g mg^{-1} min^{-1})	q_e (mg g^{-1})	R^2
5	0.123	243.08	0.9875	0.001	254.97	0.9993

order [46] kinetic models. The pseudo-first order and pseudo-second order kinetic models were given by the following equations, respectively.

$$\ln\left(q_e - q_t\right) = \ln q_e - k_1 t \tag{4}$$

$$\frac{t}{q_t} = \frac{1}{k_2 q_e^2} + \frac{t}{q_e} \tag{5}$$

where q_e (mg g^{-1}) and q_t (mg g^{-1}) are the amount of MB adsorbed on the HC5 at equilibrium and at time t (min), respectively; k_1 (min^{-1}) and k_2 (g mg^{-1} min^{-1}) are the adsorption rate constants of the pseudo-first order and pseudo-second order kinetic models, respectively.

Table 4 shows the kinetic parameters calculated from the pseudo-first order and pseudo-second order kinetic models. The correlation coefficient of the pseudo-second order model was apparently higher than that of the pseudo-first order model. On the basis of this result, the MB adsorption on HC5 was described by the pseudo-second order model.

4. Conclusion

This study successfully carbonized phenolic waste liquid via a convenient HTC process at a lower temperature (180°C) assisted by NP-10. The BET surface area of the hydrothermal carbon obtained under the optimum NP-10 dosage condition was 14.05 m^2 g^{-1}, and the adsorption capacity can reach 698 mg g^{-1} for MB adsorption, which was higher than that of the commercial AC. Therefore, the hydrochar may have great potential applications in wastewater treatment.

Acknowledgments

This work was financially supported by Shanghai Sailing Program (No.17YF1407200) and the "Capacity Building Project of Some Local Colleges and Universities in Shanghai" (No.17030501200).

References

[1] I. Azni, S. Katayon, Degradation of phenol in wastewater using anolyte produced from electrochemical generation of brine solution, Global NEST Int. J., 4 (2002) 139–144.
[2] W. Hu, Y. Gao, Treatment of phenolic wastewater by incineration, Ind. Water Waste, 31 (2000) 28–29.
[3] P. Barták, P. Frnková, L. Čáp, Determination of phenols using simultaneous steam distillation–extraction, J. Chromatogr., A, 867 (2000) 281–287.
[4] M.T.A. Reis, O.M.F. Freitas, S. Agarwal, L.M. Ferreira, M.R.C. Ismael, R. Machado, J.M.R. Carvalho, Removal of phenols from aqueous solutions by emulsion liquid membranes, J. Hazard. Mater., 192 (2011) 986–994.
[5] C. Zidi, R. Tayeb, M. Dhahbi, Extraction of phenol from aqueous solutions by means of supported liquid membrane (MLS) containing tri–noctyl phosphine oxide (TOPO), J. Hazard. Mater., 194 (2011) 62–68.
[6] R.R.N. Marques, F. Stüber, K.M. Smith, A. Fabregat, C. Bengoa, J. Font, A. Fortuny, S. Pullket, G.D. Fowler, N.J.D. Graham, Sewage sludge based catalysts for catalytic wet air oxidation of phenol: preparation, characterisation and catalytic performance, Appl. Catal., B, 101 (2011) 306–316.
[7] S. Lefèvre, O. Boutin, J.–H. Ferrasse, L. Malleret, R. Faucherand, A. Viand, Thermodynamic and kinetic study of phenol degradation by a non–catalytic wet air oxidation process, Chemosphere, 84 (2011) 1208–1215.
[8] X. Zhu, J.R. Ni, J. Wei, X. Xing, H. Li, Y. Jiang, Scale–up of BDD anode system for electrochemical oxidation of phenol simulated wastewater in continuous mode, J. Hazard. Mater., 184 (2010) 493–498.
[9] P. Jiang, J. Zhou, A. Zhang, Y. Zhong, Electrochemical degradation of p–nitrophenol with different processes, J. Environ. Sci., 22 (2010) 500–506.
[10] S. Raghu, C.A. Basha, Chemical or electrochemical techniques, followed by ion exchange, for recycle of textile dye wastewater, J. Hazard. Mater., 149 (2007) 324–330.
[11] N.D. Berge, K.S. Ro, J. Mao, J.R.V. Flora, M.A. Chappell, S. Bae, Hydrothermal carbonization of municipal waste streams, Environ. Sci. Technol., 45 (2011) 5696–5703.
[12] M.M. Titirici, A. Thomas, S. Yu, J.O. Muller, M. Antonietti, A direct synthesis of mesoporous carbons with bicontinuous pore morphology from crude plant material by hydrothermal carbonization, Chem. Mater., 19 (2007) 4205–4212.
[13] Z. Wu, C. Li, H. Liang, J. Chen, S. Yu, Ultralight, flexible, and fire–resistant carbon nanofiber aerogels from bacterial cellulose, Angew. Chem., Int. Ed., 52 (2013) 2925–2929.
[14] B. Hu, S. Yu, K. Wang, L. Liu, X Xu, Functional carbonaceous materials from hydrothermal carbonization of biomass: an effective chemical process, Dalton Trans., 40 (2008) 5414–5423.
[15] M.M. Titirici, R.J. White, C. Falco, M. Sevilla, Black perspectives for a green future: hydrothermal carbons for environment protection and energy storage, Energy Environ. Sci., 5 (2012) 6796–6822.
[16] T.P. Fellinger, R.J. White, M.M. Titirici, M. Antonietti, Borax–mediated formation of carbon aerogels from glucose, Adv. Funct. Mater., 22 (2012) 3254–3260.
[17] C. Falco, N. Baccile, M.M. Titirici, Morphological and structural differences between glucose, cellulose and lignocellulosic biomass derived hydrothermal carbons, Green Chem., 13 (2011) 3273–3281.
[18] J. Poerschmann, B. Weiner, H. Wedwitschka, A. Zehnsdorf, R. Koehler, F.D. Kopinke, Characterization of biochars and dissolved organic matter phases obtained upon hydrothermal carbonization of Elodea nuttallii, Bioresour. Technol., 189 (2015) 145–153.
[19] J. Poerschmann, B. Weiner, I. Baskyr, Organic compounds in olive mill wastewater and in solutions resulting from hydrothermal carbonization of the wastewater, Chemosphere, 92 (2013) 1472–1482.
[20] J. Poerschmann, I. Baskyr, B. Weiner, R. Koehler, H. Wedwitschka, F.D. Kopinke, Hydrothermal carbonization of olive mill wastewater, Bioresour. Technol., 133 (2013) 581–588.
[21] J. Poerschmann, B. Weiner, H. Wedwitschka, I. Baskyr, R. Koehler, F.D. Kopinke, Characterization of biocoals and dissolved organic matter phases obtained upon hydrothermal carbonization of brewer's spent grain, Bioresour. Technol., 164 (2014) 162–169.
[22] M.T. Reza, A. Freitas, X. Yang, C.J. Coronella, Wet air oxidation of hydrothermal carbonization (HTC) process liquid, ACS Sustain. Chem. Eng., 4 (2016) 3250–3254.

[23] B. Weiner, I. Baskyr, J. Poerschmann, F.D. Kopinke, Potential of the hydrothermal carbonization process for the degradation of organic pollutants, Chemosphere, 92 (2013) 674–680.
[24] S. Yin, Z. Tan, Hydrothermal liquefaction of cellulose to bio–oil under acidic, neutral and alkaline conditions, Appl. Energy, 92 (2012) 234–239.
[25] Z. Srokol, A.G. Bouche, A. Estrik, R.C.J. Strik, T. Maschmeyer, J.A. Peters, Hydrothermal upgrading of biomass to biofuel; studies on some monosaccharide model compounds, Carbohydr. Res., 339 (2004) 1717–1726.
[26] D. Esposito, M. Antonietti, Chemical conversion of sugars to lactic acid by alkaline hydrothermal processes, ChemSusChem, 6 (2013) 989–992.
[27] Y. Wang, W. Deng, B. Wang, Q. Zhang, X. Wan, Z. Tang, Y. Wang, C. Zhu, Z. Cao, G. Wang, H. Wan, Chemical synthesis of lactic acid from cellulose catalysed by lead (II) ions in water, Nat. Commun., 4 (2013) 2141–2147.
[28] H. Zhao, J.E. Holladay, H. Brown, Z. Zhang, Metal chlorides in ionic liquid solvents convert sugars to 5–hydroxymethylfurfural, Science, 316 (2007) 1597–1600.
[29] L. Peng, L. Lin, J. Zhang, J. Zhuang, B. Zhang, Y. Gong, Catalytic conversion of cellulose to levulinic acid by metal chlorides, Molecules, 15 (2010) 5258–5272.
[30] Z. Ding, J. Shi, J. Xiao, W. Gu, C. Zheng, H. Wang, Catalytic conversion of cellulose to 5–hydroxymethyl furfural using acidic ionic liquids and co–catalyst, Carbohydr. Polym., 90 (2012) 792– 798.
[31] S.B.A. Hamid, S.J. Teh, Y.S. Lim. Catalytic hydrothermal upgrading of α–cellulose using iron salts as a Lewis acid, Bioresources, 10 (2015) 5974–5986.
[32] J. Hao, W. Zhang, G. Xue, P. Rao, R. Wang, Treatment of distillation residue waste liquid from NPEOs by hydrothermal carbonization process for resource recovery, Desal. Wat. Treat., 125 (2018) 26–31.
[33] State Environmental Protection Administration of China, Water and Wastewater Monitoring and Analysis Methods, 4th ed., China Environmental Science Press, Beijing, 2002, pp. 210–213.
[34] S. Sivrikaya, S. Albayrak, M. Imamoglu, A. Gundogdu, C. Duran, H. Yildiz, Dehydrated hazelnut husk carbon: a novel sorbent for removal of Ni (II) ions from aqueous solution, Desal. Wat. Treat., 50 (2012) 2–13.
[35] M. Kruk, M. Jaroniec, Gas adsorption characterization of ordered organic–inorganic nanocomposite materials, Chem. Mater., 13 (2001) 3169–3183.
[36] L. Gu, B. Li, H. Wen, X. Zhang, L. Wang, J. Ye, Co-hydrothermal treatment of fallen leaves with iron sludge to prepare magnetic iron product and solid fuel, Bioresour. Technol., 257 (2018) 229–237.
[37] S. Kang, X. Li, J. Fan, J. Chang, Characterization of hydrochars produced by hydrothermal carbonization of lignin, cellulose, D–xylose, and wood meal, Ind. Eng. Chem. Res., 51 (2012) 9023–9031.
[38] H. Deng, L. Yang, G. Tao, J. Dai, Preparation and characterization of activated carbon from cotton stalk by microwave assisted chemical activation–application in methylene blue adsorption from aqueous solution, J. Hazard. Mater., 166 (2009) 1514–1521.
[39] V. Boonamnuayvitaya, S. Ung–Sae, W. Tanthapanichakoon, Preparation of activated carbons from coffee residue for the adsorption of formaldehyde, Sep. Purif. Technol., 42 (2005) 159–168.
[40] W. Shen, Z. Li, Y. Liu, Surface chemical functional groups modification of porous carbon, Recent Pat. Chem. Eng., 1 (2008) 27–40.
[41] J. Mosa, A. Durán, M. Aparicio, Sulfonic acid–functionalized 294 hybrid organic–inorganic proton exchange membranes synthesized by sol–gel using 3–mercaptopropyl trimethoxysilane (MPTMS), J. Power Sources, 297 (2015) 208–216.
[42] I. Langmuir, The adsorption of gases on plane surfaces of glass, mica and platinum, J. Am. Chem. Soc., 40 (1918) 1361–1403.
[43] H.M.F. Freundlich, Uber die adsorption in losungen, Z. Phys. Chem., 57 (1906) 385–470.
[44] O. Kazaka, Y.R. Ekerb, I. Akinc, H. Bingold, A. Tora, A novel red mud@sucrose based carbon composite: preparation, characterization and its adsorption performance toward methylene blue in aqueous solution, J. Environ. Chem. Eng., 5 (2017) 2639–2647.
[45] S. Lagergren, About the theory of so–called adsorption of soluble substances, K. Sven. Vetensk. Handl., 24 (1898) 1–39.
[46] Y. Ho, G. McKay, Pseudo–second order model for sorption processes, Process Biochem., 34 (1999) 451–465.